

Compact formulation of the beam shape coefficients for elliptical Gaussian beam based on localized approximation

JIANQI SHEN,* XIAOWEI JIA, AND HAITAO YU

University of Shanghai for Science and Technology, Shanghai 200093, China

*Corresponding author: jqshen@163.com

Received 22 August 2016; revised 9 October 2016; accepted 9 October 2016; posted 10 October 2016 (Doc. ID 274137); published 28 October 2016

It has been proved that localized approximation (LA) is the most efficient way to evaluate the beam shape coefficients (BSCs) in generalized Lorenz–Mie theory. The BSCs are usually expressed in the form of multiple summations of an infinite series of terms, which is cumbersome to calculate, and the infinite series is frequently slowly convergent. In this paper, we present a compact expression of the BSCs for an elliptical Gaussian beam based on the LA that is more convenient and efficient for numerical computations. A comparison with the integral LA is made, showing the reliability, stability, and efficiency of the presented formulation. © 2016 Optical Society of America

OCIS codes: (290.4020) Mie theory; (140.3295) Laser beam characterization.

<http://dx.doi.org/10.1364/JOSAA.33.002256>

1. INTRODUCTION

Historically, with the laser coming out and the broad application in the field of optical particle characterization [1], the classical Lorenz–Mie theory failed to accurately describe the scattering characteristics of the scatterers, which spawned the development of the generalized Lorenz–Mie theory (GLMT). During the last three decades and more, the GLMT has been developed to a state of maturity through unremitting efforts of members of the light-scattering community worldwide [2–7].

The core problem in GLMT lies in the evaluation of the beam shape coefficients (BSCs). The BSCs can be evaluated by using quadrature [8–10], finite series [11,12], localized approximation (LA) and its modified versions [13–22], and integral localized approximation (ILA) [23]. Historically, the first method to evaluate BSCs was that of using quadrature. This method is flexible because only kernels have to be changed when the description of the illuminating beam is changed. However, it is time consuming due to the spherical Bessel functions and associated Legendre functions involved in the integrands possess complex oscillatory behaviors. The LA is time saving; however, it is not flexible. The integral localized approximation holds the advantages of flexibility, high speed, and stability. Actually, the essential distinction between the ILA and the LA is that the former keeps the form of the integral over the azimuthal angle but the latter transforms this integral into a form of multiple summations of infinite series of terms for a certain shaped beam. Within the ILA, the variation of

integrand via ϕ is strongly oscillating especially when the index of the azimuthal mode is large. From the viewpoint of numerical integral, subtraction between large numbers may result in loss of significant digits in the computation of BSCs.

The localized beam models go through a process of continuous improvement and perfectness before maturity; see [4,22,24] and references therein. Different versions have been developed, such as the original localized approximation (OLA) [14] and the modified localized approximation (MLA) [16,17,19,21,22]. Usually, the BSCs for a certain shaped beam are expressed in terms of double (or triple and even quadruple) summations of infinite series of terms depending on the characteristics of the beam [21,22,25], which is cumbersome to calculate, and the infinite series is frequently slowly convergent. It was observed from numerical calculations that the LA lacks stability when the partial wave number n becomes high [23]. Nevertheless, there is some evidence showing that the expression of the BSCs obtained with the LA can be further simplified so as to speed up and stabilize the numerical calculation, at least for some special beams. One example is given by Lock [18], in which a compact formulation of the BSCs is derived for a circular Gaussian beam. Another example is the evaluation of the BSCs of a high-order Bessel beam [26,27]. In these examples, the BSCs are given in terms of Bessel functions or modified Bessel functions.

The objective of this paper is to derive a compact formulation of the BSCs for an elliptical Gaussian beam based on the LA method. The elliptical Gaussian beam is also called laser

sheet. Most laser diodes or solid-state lasers emit elliptical Gaussian beams. In addition, the elliptical Gaussian beam can also be transformed from a circular Gaussian beam by using a cylindrical lens. The use of elliptical Gaussian beams is of growing interest in measurement techniques relying on light scattering, such as optical sizing, particle image velocimetry, and optical trapping and manipulation [28–31]. The paper is organized as follows. Section 2 derives the formulation of the BSCs for an elliptical Gaussian beam together with a discussion of some special cases. Section 3 exemplifies some numerical results, showing a comparison with the ILA. Section 4 is devoted to the conclusion.

2. LOCALIZED APPROXIMATION OF AN ELLIPTICAL GAUSSIAN BEAM

The GLMT uses two Cartesian coordinate systems, O_{Buvw} and O_pxyz , with parallel axes for a standard configuration, as indicated in Fig. 1, and a spherical coordinate system, (r, θ, ϕ) , based on O_pxyz . The coordinate O_pxyz is attached to a regularly shaped particle, such as the spherical or spheroidal particle, whose center is located at O_p . The coordinate system O_{Buvw} is attached to the illuminating shaped beam and the beam center is located at O_B . The beam propagates along the positive w axis. The coordinates of O_B with respect to O_pxyz are denoted (x_0, y_0, z_0) .

$$\begin{cases} E_r = E_0 \psi_0^{\text{sh}} \left(\cos \phi \sin \theta - \frac{2Q_x}{k\omega_{0x}^2} \cos \theta (r \cos \phi \sin \theta - x_0) \right) \exp(-ikr \cos \theta + ikz_0) \\ H_r = H_0 \psi_0^{\text{sh}} \left(\sin \phi \sin \theta - \frac{2Q_y}{k\omega_{0y}^2} \cos \theta (r \sin \phi \sin \theta - y_0) \right) \exp(-ikr \cos \theta + ikz_0) \end{cases} \quad (6)$$

The procedure to obtain the expressions of the BSCs in the framework of the localized approximation is described in [13,14] for Gaussian beams and later it is applied to other beams [20,25]. It starts by expanding the radial electric and magnetic fields into azimuthal modes, according to

$$\begin{cases} E_r = \sum_m E_r^m \\ H_r = \sum_m H_r^m \end{cases} \quad (1)$$

A flexible method to extract the azimuthal modes from the radial fields is introduced in [23] by using the relation

$$\int_0^{2\pi} \exp[i(m - m')\phi] d\phi = 2\pi \delta_{mm'}, \quad (2)$$

and the azimuthal modes are obtained with

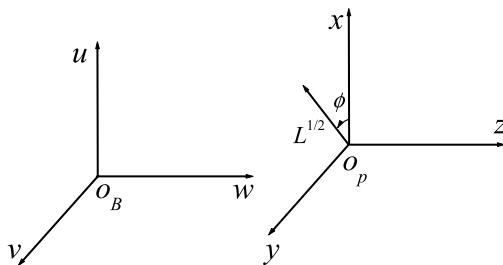


Fig. 1. Geometry of the GLMT.

$$\begin{cases} E_r^m = \exp(im\phi) \frac{1}{2\pi} \int_0^{2\pi} E_r(r, \theta, \phi') \exp(-im\phi') d\phi' \\ H_r^m = \exp(im\phi) \frac{1}{2\pi} \int_0^{2\pi} H_r(r, \theta, \phi') \exp(-im\phi') d\phi' \end{cases} \quad (3)$$

The BSCs are then evaluated by [25]

$$\begin{cases} \tilde{g}_{n, TM}^m = \frac{Z_n^m}{2\pi E_0} \int_0^{2\pi} \hat{G}\{E_r(r, \theta, \phi)\} \exp(-im\phi) d\phi \\ \tilde{g}_{n, TE}^m = \frac{Z_n^m}{2\pi H_0} \int_0^{2\pi} \hat{G}\{H_r(r, \theta, \phi)\} \exp(-im\phi) d\phi \end{cases} \quad (4)$$

in which the bar designates the localized approximation. The localization operator \hat{G} changes the radial parameter kr to $L^{1/2}$ and the polar angle θ to $\pi/2$. Here, $k = 2\pi/\lambda$ is the wave number and λ is the wavelength, $L^{1/2} = n + 0.5$ in the OLA and $L = (n + 0.5)^2 - (|m| + 0.5)^2$ in the MLA [16,17]. The normalization factors are given as [22]

$$Z_n^m = \begin{cases} \frac{n(n+1)i}{n+0.5} & m = 0 \\ \left(\frac{-i}{L^{1/2}}\right)^{|m|-1} & m \neq 0 \end{cases} \quad (5)$$

An approximate description of laser sheets is introduced and the involved approximation order is discussed in Cartesian and spherical coordinate systems in [32]. The radial components of the electromagnetic field, in the time convention $\exp(i\omega t)$, are given as

where

$$\begin{aligned} \psi_0^{\text{sh}} = i\sqrt{Q_x Q_y} \exp \left\{ -\frac{iQ_x}{\omega_{0x}^2} (r \cos \phi \sin \theta - x_0)^2 \right. \\ \left. - \frac{iQ_y}{\omega_{0y}^2} (r \sin \phi \sin \theta - y_0)^2 \right\}, \end{aligned} \quad (7)$$

$$\begin{cases} Q_x = [i + 2(r \cos \theta - z_0)/k\omega_{0x}^2]^{-1} \\ Q_y = [i + 2(r \cos \theta - z_0)/k\omega_{0y}^2]^{-1} \end{cases} \quad (8)$$

in which ω_{0x} and ω_{0y} are the beam waist radii along the x - and y -axes, respectively. The parameter ψ_0^{sh} is taken as a product of two factors, i.e., $\psi_0^{\text{sh}} = \psi_0^{0, \text{sh}} \psi_0^{\phi, \text{sh}}$:

$$\begin{aligned} \psi_0^{0, \text{sh}} = i\sqrt{Q_x Q_y} \exp \left[\frac{-i}{2} \left(\frac{Q_x}{\omega_{0x}^2} + \frac{Q_y}{\omega_{0y}^2} \right) r^2 \sin^2 \theta \right. \\ \left. - i \left(\frac{Q_x}{\omega_{0x}^2} x_0^2 + \frac{Q_y}{\omega_{0y}^2} y_0^2 \right) \right], \end{aligned} \quad (9)$$

$$\begin{aligned} \psi_0^{\phi, \text{sh}} = \exp \left\{ A[\exp(i2\phi) + \exp(-i2\phi)] \right. \\ \left. + 2i \left(\frac{Q_x}{\omega_{0x}^2} x_0 \cos \phi + \frac{Q_y}{\omega_{0y}^2} y_0 \sin \phi \right) r \sin \theta \right\}, \end{aligned} \quad (10)$$

in which $\psi_0^{\phi, \text{sh}}$ is ϕ -dependent but $\psi_0^{0, \text{sh}}$ is not. The parameter A denotes the nonaxisymmetry of the beam, defined by

$$A = -\frac{r^2 \sin^2 \theta}{4} \left(\frac{iQ_x}{\omega_{0x}^2} - \frac{iQ_y}{\omega_{0y}^2} \right). \quad (11)$$

Following the same spirit of the localized approximation as for the Gaussian beam, the BSCs are obtained in terms of triple summations [25] that are later proved to be unstable in numerical computation [23]. The following procedure of derivation is slightly different from that in [25], which allows us to obtain a more concise formulation of the BSCs. Applying the localization operator \hat{G} to the radial components of the beam fields, we have

$$\begin{cases} \hat{G}\{E_r\} = E_0 \tilde{\psi}_0^{0,\text{sh}} \tilde{\psi}_0^{\phi,\text{sh}} \cos \phi \\ \hat{G}\{H_r\} = H_0 \tilde{\psi}_0^{0,\text{sh}} \tilde{\psi}_0^{\phi,\text{sh}} \sin \phi \end{cases} \quad (12)$$

$$\begin{aligned} \tilde{\psi}_0^{0,\text{sh}} &= i\sqrt{\bar{Q}_x \bar{Q}_y} \exp[iZ_0 - \frac{i}{2}(\bar{Q}_x s_x^2 + \bar{Q}_y s_y^2)L \\ &\quad - i(\bar{Q}_x s_x^2 X_0^2 + \bar{Q}_y s_y^2 Y_0^2)], \end{aligned} \quad (13)$$

$$\tilde{\psi}_0^{\phi,\text{sh}} = \exp\{\bar{A}[\exp(i2\phi) + \exp(-i2\phi)] + iF \sin(\phi + \xi)\}, \quad (14)$$

$$\begin{cases} \bar{Q}_x = (i - 2Z_0 s_x^2)^{-1} \\ \bar{Q}_y = (i - 2Z_0 s_y^2)^{-1} \end{cases}, \quad (15)$$

$$\bar{A} = -\frac{iL}{4}(\bar{Q}_x s_x^2 - \bar{Q}_y s_y^2), \quad (16)$$

in which $(X_0, Y_0, Z_0) = (kx_0, ky_0, kz_0)$, $s_x = 1/k\omega_{0x}$, and $s_y = 1/k\omega_{0y}$ are dimensionless beam confinement parameters along the x - and y -axes. \bar{F} and ξ are defined by

$$\bar{F} = 2L^{1/2} \sqrt{(\bar{Q}_x s_x^2 X_0)^2 + (\bar{Q}_y s_y^2 Y_0)^2}, \quad (17)$$

$$\begin{cases} \sin \xi = \frac{\bar{Q}_x s_x^2 X_0}{\sqrt{(\bar{Q}_x s_x^2 X_0)^2 + (\bar{Q}_y s_y^2 Y_0)^2}} \\ \cos \xi = \frac{\bar{Q}_y s_y^2 Y_0}{\sqrt{(\bar{Q}_x s_x^2 X_0)^2 + (\bar{Q}_y s_y^2 Y_0)^2}} \end{cases}. \quad (18)$$

The factor $\tilde{\psi}_0^{\phi,\text{sh}}$ in Eq. (14) can be further expanded into a Fourier expansion, read as

$$\tilde{\psi}_0^{\phi,\text{sh}} = \sum_{p,q=0}^{\infty} \frac{\bar{A}^{p+q}}{p!q!} e^{i\phi(2p-2q)} \exp\{i\bar{F} \sin(\phi + \xi)\}. \quad (19)$$

Inserting Eq. (12) into Eq. (4) and using the $\tilde{\psi}_0^{\phi,\text{sh}}$ given in Eq. (19), we obtain the BSCs as

$$\begin{cases} \tilde{g}_{n,\text{TM}}^m = \frac{1}{2} Z_n^m \tilde{\psi}_0^{0,\text{sh}} \sum_{p,q=0}^{\infty} \frac{\bar{A}^{p+q}}{p!q!} \left\{ \frac{1}{2\pi} \int_0^{2\pi} \exp[i\bar{F} \sin(\phi + \xi) + i(2p-2q+1-m)\phi] d\phi \right. \\ \quad \left. + \frac{1}{2\pi} \int_0^{2\pi} \exp[i\bar{F} \sin(\phi + \xi) + i(2p-2q-1-m)\phi] d\phi \right\} \\ \tilde{g}_{n,\text{TE}}^m = \frac{1}{2i} Z_n^m \tilde{\psi}_0^{0,\text{sh}} \sum_{p,q=0}^{\infty} \frac{\bar{A}^{p+q}}{p!q!} \left\{ \frac{1}{2\pi} \int_0^{2\pi} \exp[i\bar{F} \sin(\phi + \xi) + i(2p-2q+1-m)\phi] d\phi \right. \\ \quad \left. - \frac{1}{2\pi} \int_0^{2\pi} \exp[i\bar{F} \sin(\phi + \xi) + i(2p-2q-1-m)\phi] d\phi \right\} \end{cases}. \quad (20)$$

By using the definition of the Bessel function,

$$J_p(u) = \frac{1}{2\pi} \int_0^{2\pi} \exp[i(p\phi - u \sin \phi)] d\phi, \quad (21)$$

Eq. (20) can be further developed into

$$\begin{cases} \tilde{g}_{n,\text{TM}}^m = \frac{1}{2} Z_n^m \tilde{\psi}_0^{0,\text{sh}} \cdot T^+ \\ \tilde{g}_{n,\text{TE}}^m = \frac{1}{2i} Z_n^m \tilde{\psi}_0^{0,\text{sh}} \cdot T^- \end{cases}, \quad (22)$$

where

$$T^\pm = \sum_{p,q=0}^{\infty} \frac{\bar{A}^{p+q}}{p!q!} \{ \tilde{J}_{m-1-2p+2q}(\bar{F}) \pm \tilde{J}_{m+1-2p+2q}(\bar{F}) \}. \quad (23)$$

Here, $\tilde{J}_p(\bar{F}) = e^{ip\xi} J_p(\bar{F})$ is used for simplicity of expression. Equation (23) can be further simplified by splitting it into three parts. The first part contains those terms satisfying $p = q$, which leads to

$$T_{p=q}^\pm = \sum_{p=0}^{\infty} \left(\frac{\bar{A}^p}{p!} \right)^2 \{ \tilde{J}_{m-1}(\bar{F}) \pm \tilde{J}_{m+1}(\bar{F}) \}. \quad (24)$$

The other two parts are those for $p > q$ and $p < q$:

$$\begin{cases} T_{p<q}^\pm = \sum_{p=0}^{\infty} \sum_{q=p}^{\infty} \frac{\bar{A}^{p+q}}{p!q!} \{ \tilde{J}_{m-1-2p+2q}(\bar{F}) \pm \tilde{J}_{m+1-2p+2q}(\bar{F}) \} \\ T_{p>q}^\pm = \sum_{q=0}^{\infty} \sum_{p=q}^{\infty} \frac{\bar{A}^{p+q}}{p!q!} \{ \tilde{J}_{m-1-2p+2q}(\bar{F}) \pm \tilde{J}_{m+1-2p+2q}(\bar{F}) \} \end{cases}. \quad (25)$$

Letting $s = q - p$ and $t = p - q$, and then changing the order of summations, Eq. (25) can be written as

$$\begin{aligned} T_{p<q}^\pm &= \sum_{s=1}^{\infty} \{ \tilde{J}_{m-1+2s}(\bar{F}) \pm \tilde{J}_{m+1+2s}(\bar{F}) \} \sum_{p=0}^{\infty} \frac{\bar{A}^{2p+s}}{p!(s+p)!} \\ T_{p>q}^\pm &= \sum_{t=1}^{\infty} \{ \tilde{J}_{m-1-2t}(\bar{F}) \pm \tilde{J}_{m+1-2t}(\bar{F}) \} \sum_{q=0}^{\infty} \frac{\bar{A}^{2q+t}}{(t+q)!q!}. \end{aligned} \quad (26)$$

Employing the definition of the modified Bessel function, i.e.,

$$I_p(u) = \sum_{k=0}^{\infty} \frac{(u/2)^{p+2k}}{k!(p+k)!},$$

$$\begin{cases} T_{p=q}^\pm = I_0(2\bar{A}) \{ \tilde{J}_{m-1}(\bar{F}) \pm \tilde{J}_{m+1}(\bar{F}) \} \\ T_{p<q}^\pm = \sum_{s=1}^{\infty} I_s(2\bar{A}) \{ \tilde{J}_{m-1+2s}(\bar{F}) \pm \tilde{J}_{m+1+2s}(\bar{F}) \} \\ T_{p>q}^\pm = \sum_{t=1}^{\infty} I_t(2\bar{A}) \{ \tilde{J}_{m-1-2t}(\bar{F}) \pm \tilde{J}_{m+1-2t}(\bar{F}) \} \end{cases}. \quad (27)$$

Therefore, the final solution of the BSCs is obtained:

$$\begin{cases} \tilde{g}_{n,\text{TM}}^m = \frac{1}{2} Z_n^m \tilde{\psi}_0^{0,\text{sh}} \cdot \left\{ I_0(2\bar{A}) [\tilde{J}_{m-1}(\bar{F}) + \tilde{J}_{m+1}(\bar{F})] + \sum_{s=1}^{\infty} I_s(2\bar{A}) [\tilde{J}_{m+2s-1}(\bar{F}) + \tilde{J}_{m-2s-1}(\bar{F}) + \tilde{J}_{m+2s+1}(\bar{F}) + \tilde{J}_{m-2s+1}(\bar{F})] \right\} \\ \tilde{g}_{n,\text{TE}}^m = \frac{1}{2i} Z_n^m \tilde{\psi}_0^{0,\text{sh}} \cdot \left\{ I_0(2\bar{A}) [\tilde{J}_{m-1}(\bar{F}) - \tilde{J}_{m+1}(\bar{F})] + \sum_{s=1}^{\infty} I_s(2\bar{A}) [\tilde{J}_{m+2s-1}(\bar{F}) + \tilde{J}_{m-2s-1}(\bar{F}) - \tilde{J}_{m+2s+1}(\bar{F}) - \tilde{J}_{m-2s+1}(\bar{F})] \right\} \end{cases}. \quad (28)$$

Or by using the relation $I_p(u) = (-i)^p J_p(iu)$, we have

$$\begin{cases} \tilde{g}_{n,\text{TM}}^m = \frac{1}{2} Z_n^m \tilde{\psi}_0^{0,\text{sh}} \cdot \left\{ J_0(\tilde{D}) [\tilde{J}_{m-1}(\tilde{F}) + \tilde{J}_{m+1}(\tilde{F})] + \sum_{s=1}^{\infty} (-i)^s J_s(\tilde{D}) [\tilde{J}_{m+2s-1}(\tilde{F}) + \tilde{J}_{m-2s-1}(\tilde{F}) + \tilde{J}_{m+2s+1}(\tilde{F}) + \tilde{J}_{m-2s+1}(\tilde{F})] \right\} \\ \tilde{g}_{n,\text{TE}}^m = \frac{1}{2i} Z_n^m \tilde{\psi}_0^{0,\text{sh}} \cdot \left\{ J_0(\tilde{D}) [\tilde{J}_{m-1}(\tilde{F}) - \tilde{J}_{m+1}(\tilde{F})] + \sum_{s=1}^{\infty} (-i)^s J_s(\tilde{D}) [\tilde{J}_{m+2s-1}(\tilde{F}) + \tilde{J}_{m-2s-1}(\tilde{F}) - \tilde{J}_{m+2s+1}(\tilde{F}) - \tilde{J}_{m-2s+1}(\tilde{F})] \right\} \end{cases} \quad (29)$$

in which

$$\tilde{D} = 2i\tilde{A} = \frac{L}{2} (\tilde{Q}_x s_x^2 - \tilde{Q}_y s_y^2). \quad (30)$$

Compared with the expression obtained in [25], Eq. (29) is more compact and very easy for numerical computation.

Special Case I: Gaussian Beam, Off-axis Location

The Gaussian beam case can be recovered as a special case of the elliptical Gaussian beam (laser sheet) when $\omega_{0x} = \omega_{0y} = \omega_0$. This leads to $\tilde{D} = 0$ so that the BSCs described in Eqs. (29) and (30) read as

$$\begin{cases} \tilde{g}_{n,\text{TM}}^m = \frac{1}{2} Z_n^m \tilde{\psi}_0^0 \cdot \{ \tilde{J}_{m-1}(\tilde{F}) + \tilde{J}_{m+1}(\tilde{F}) \} \\ \tilde{g}_{n,\text{TE}}^m = \frac{1}{2i} Z_n^m \tilde{\psi}_0^0 \cdot \{ \tilde{J}_{m-1}(\tilde{F}) - \tilde{J}_{m+1}(\tilde{F}) \} \end{cases} \quad (31)$$

$$\tilde{\psi}_0^0 = i\tilde{Q} \exp\{iZ_0 - i\tilde{Q}s^2(L + X_0^2 + Y_0^2)\}, \quad (32)$$

$$\tilde{F} = 2L^{1/2}\tilde{Q}s^2\sqrt{X_0^2 + Y_0^2}, \quad (33)$$

where $\tilde{Q} = (i - 2Z_0 s^2)^{-1}$ and $s = 1/k\omega_0$. Equations (31)–(33) are equivalent to the compact formulations derived in [18], although they are slightly different in form due to the difference of the time convention and the definition of the BSCs [33].

A more special case is the on-axis location for the Gaussian beam when $X_0^2 + Y_0^2 = 0$ and hence $\tilde{F} = 0$. In this case, all the BSCs are equal to zero except for those $|m| = 1$.

Special Case II: Elliptical Gaussian Beam, On-axis Case

The on-axis case for an elliptical Gaussian beam is characterized by $\omega_{0x} \neq \omega_{0y}$ and $X_0^2 + Y_0^2 = 0$, which leads to $\tilde{D} \neq 0$ and $\tilde{F} = 0$. In this case, the BSCs can be simplified from Eq. (29) to

$$\begin{cases} \tilde{g}_{n,\text{TM}}^m = \frac{1}{2} Z_n^m \tilde{\psi}_0^{0,\text{sh}} \cdot \left[J_0(\tilde{D}) (\delta_{m,1} + \delta_{m,-1}) + \sum_{s=1}^{\infty} (-i)^s J_s(\tilde{D}) (\delta_{2s,1-m} + \delta_{2s,m-1} + \delta_{2s,-1-m} + \delta_{2s,1+m}) \right] \\ \tilde{g}_{n,\text{TE}}^m = \frac{1}{2i} Z_n^m \tilde{\psi}_0^{0,\text{sh}} \cdot \left[J_0(\tilde{D}) (\delta_{m,1} - \delta_{m,-1}) + \sum_{s=1}^{\infty} (-i)^s J_s(\tilde{D}) (\delta_{2s,1-m} + \delta_{2s,m-1} - \delta_{2s,-1-m} - \delta_{2s,1+m}) \right] \end{cases} \quad (34)$$

It is easy to find that all the BSCs of the even azimuthal modes are equal to zero (i.e., $\tilde{g}_{n,\text{TM}}^{2p} = \tilde{g}_{n,\text{TE}}^{2p} = 0$) and all the BSCs of the odd azimuthal modes satisfy the relations $\tilde{g}_{n,\text{TM}}^m = \tilde{g}_{n,\text{TM}}^m$ and $\tilde{g}_{n,\text{TE}}^m = -\tilde{g}_{n,\text{TE}}^m$. For the positive odd azimuthal modes (say $m = 2p + 1$ and $p \geq 0$), we have

$$\begin{cases} \tilde{g}_{n,\text{TM}}^{2p+1} = \frac{(-i)^p}{2} Z_n^{2p+1} \tilde{\psi}_0^{0,\text{sh}} \cdot \{ J_p(\tilde{D}) - iJ_{p+1}(\tilde{D}) \} \\ \tilde{g}_{n,\text{TE}}^{2p+1} = \frac{(-i)^{p+1}}{2} Z_n^{2p+1} \tilde{\psi}_0^{0,\text{sh}} \cdot \{ J_p(\tilde{D}) + iJ_{p+1}(\tilde{D}) \} \end{cases} \quad (35)$$

3. NUMERICAL EXAMPLES AND DISCUSSION

Numerical calculation is implemented in the frame of OLA, by constructing a C++ program for the evaluation of the

BSCs of the elliptical Gaussian beam given in Eq. (29). In order to make a comparison with the ILA method, we also construct a C++ program using the adaptive Simpson's method to compute the integral of Eq. (4), which is modified to

$$\begin{pmatrix} \tilde{g}_{n,\text{TM}}^m \\ \tilde{g}_{n,\text{TE}}^m \end{pmatrix} = \frac{Z_n^m}{2\pi} \int_0^{2\pi} \tilde{\psi}_0^{\text{sh}} \begin{pmatrix} \cos \phi \\ \sin \phi \end{pmatrix} \exp(-im\phi) d\phi, \quad (36)$$

$$\tilde{\psi}_0^{\text{sh}} = i\sqrt{\tilde{Q}_x \tilde{Q}_y} \exp \left\{ \begin{matrix} iZ_0 - i\tilde{Q}_x s_x^2 (L^{1/2} \cos \phi - X_0)^2 \\ -i\tilde{Q}_y s_y^2 (L^{1/2} \sin \phi - Y_0)^2 \end{matrix} \right\}. \quad (37)$$

In the first part of the numerical computation, we use the parameters of the elliptical Gaussian beam of [23], namely, $\lambda = 0.5145 \mu\text{m}$ (the argon laser), $\omega_{0x} = 3 \text{ mm}$, and $\omega_{0y} = 2 \mu\text{m}$. The corresponding confinement parameters along the x - and y -axes are $s_x = 5.5 \times 10^{-5}$ and $s_y = 4.1 \times 10^{-2}$ to which the localized approximation based on the Davis first-order approximation can be applied [16,17]. The parameters of the beam's location are $x_0 = y_0 = 0$ and $z_0 = 0.2 \text{ mm}$ for the on-axis case and $x_0 = 0$, $y_0 = 16.5 \mu\text{m}$, and $z_0 = 0.2 \text{ mm}$ for the off-axis case. Numerical results are shown in Figs. 2 and 3, which show a complete match between the LA and the ILA methods. And these results agree well with Figs. 3 and 4 of [23]. Computation of the results in Fig. 2 costs about 0.17 s for the ILA (five designed significant digits) and 0.045 s for the LA, on a personal computer powered by a 3.2 GHz CPU. The computation of Fig. 3 costs 0.12 s and 0.046 s, respectively. This means the LA is about 3 times faster than the ILA.

It is found that, for the parameters used in the above examples, the ILA can compute the BSCs for the low azimuthal modes (say $|m| < 15$) and obtain reasonable results. However, the ILA computation of the BSCs with higher azimuthal modes is extremely slow. It is evident that $\tilde{\psi}_0^{\text{sh}} \cos \phi$ or $\tilde{\psi}_0^{\text{sh}} \sin \phi$ change slowly via the variation of the azimuthal angle ϕ but $\exp(-im\phi)$ oscillates very fast for the high azimuthal mode number m . According to Simpson's rule, more points are required for the convergence of the integral if the integrand is strongly oscillatory, which slows down the computation speed. In addition, the integral in Eq. (36) decreases gradually when the azimuthal mode number increases and so do the

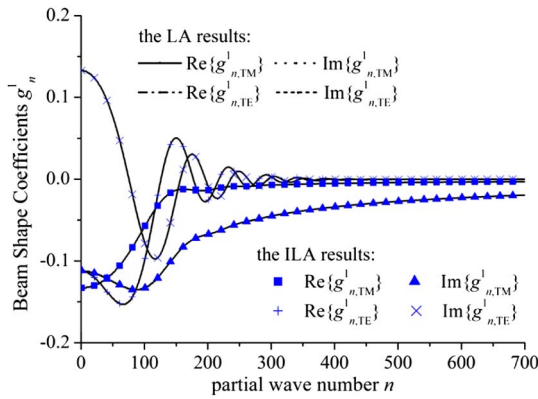


Fig. 2. Results of \bar{g}_n^1 computed by the LA (labeled with lines) and ILA (labeled with dots) for $\lambda = 0.5145 \mu\text{m}$, $\omega_{0x} = 3 \text{ mm}$, $\omega_{0y} = 2 \mu\text{m}$, $x_0 = 0$, $y_0 = 16.5 \mu\text{m}$, and $z_0 = 0.2 \text{ mm}$.

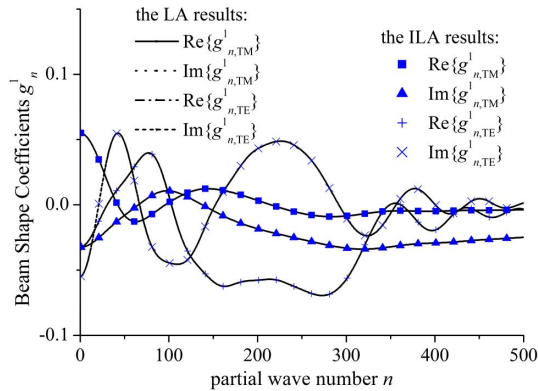


Fig. 3. Results of \bar{g}_n^1 computed by the LA (labeled with lines) and ILA (labeled with dots) for $\lambda = 0.5145 \mu\text{m}$, $\omega_{0x} = 3 \text{ mm}$, $\omega_{0y} = 2 \mu\text{m}$, $x_0 = y_0 = 0$, and $z_0 = 0.2 \text{ mm}$.

BSCs. This means the result is a subtraction between some large values, which leads to the loss of significant digits. For example, the double precise corresponds to 15 significant digits. If the value of the integral is 10 orders less than the maximum of the integrand, the integral computation with the five

designed significant digits will not converge. A numerical example of the BSC $|\bar{g}_{n,\text{TM}}^m|$ computed with the ILA is shown in Table 1, making a comparison with the maxima of the integrand:

$$I_{nm,\text{TM}} = \max \left| \frac{Z_n^m}{2\pi} e^{iZ_0} \tilde{\psi}_0^{\text{sh}} \sin \phi \exp(-im\phi) \right|. \quad (38)$$

In this computation, we use the same parameters of Fig. 2 and the partial wave number is $n = 50$. The integration is extremely slow for those high azimuth modes when $|\bar{g}_{n,\text{TM}}^m| < 10^{-10} I_{nm,\text{TM}}$. We also construct another C++ program for the ILA calculation of the BSCs, wherein the adaptive Simpson's method is replaced by the adaptive Gaussian–Kronrod quadrature method. However, this does not improve the situation.

Evaluation of BSCs with the LA relies on the computation of the Bessel functions of the first kind for integer orders and complex argument, $J_p(u)$. Since the Bessel functions satisfying the relationship $J_{-p}(u) = (-1)^p J_p(u)$, only those functions of positive orders are computed. When the argument is very small, e.g., $|u| \leq 2\sqrt{p}$, the Bessel function can be computed by using the Taylor series expansion due to its fast convergent speed. For large argument (say $|u| \geq p^2/4$), the Bessel function can be computed by the Hankel's asymptotic expansion [34], which is expanded into the reciprocal form of the argument u . Alternatively, the Bessel functions can be computed by using the downward recurrence starting from two consecutive high orders [35–37]. The values of the starting orders can be arbitrarily chosen, e.g., $J_{q+1} = 0$ and $J_q = \epsilon_1 + i\epsilon_2$, where ϵ_1 and ϵ_2 are small values. According to Toit's work [35–37], the starting point should be high enough so that the recurrence converges to the correct values soon. Since the starting values of the Bessel functions are arbitrarily chosen, the normalization must be applied to the resultant values. A proper choice of the method for computing the Bessel function may speed up the evaluation of the BSCs.

It should be noted that, if the imaginary part of the argument (i.e., $|\text{Im}(u)|$) is very big, the Bessel function of low orders $J_p(u)$ may overflow. This may happen in the evaluation of the BSCs in some exotic cases, since the arguments \bar{F} and \bar{D} are proportional to $(n + 0.5)$ and its square, respectively [see Eqs. (30) and (33)]. In order to prevent the overflow, we prefer

Table 1. Comparison between the BSCs $|\bar{g}_{n,\text{TM}}^m|$ and the Maxima of the Integrand $I_{nm,\text{TM}}^a$

Azimuth Mode Number m	BSC $ \bar{g}_{n,\text{TM}}^m $	Max. $I_{nm,\text{TM}}$	$ \bar{g}_{n,\text{TM}}^m /I_{nm,\text{TM}}$	Speed (ms)
1	1.143615×10^{-02}	3.106450×10^{-02}	3.681421×10^{-01}	0.056
3	1.625821×10^{-05}	1.244003×10^{-05}	1.306927	0.083
5	3.386650×10^{-09}	4.844763×10^{-09}	6.990333×10^{-01}	0.109
7	2.504262×10^{-13}	1.895064×10^{-12}	1.321466×10^{-01}	0.109
9	1.037864×10^{-17}	7.486012×10^{-16}	1.386405×10^{-02}	0.108
11	2.898632×10^{-22}	2.957915×10^{-19}	9.799578×10^{-04}	0.109
13	6.012181×10^{-27}	1.157939×10^{-22}	5.192142×10^{-05}	0.109
15	9.829389×10^{-32}	4.529312×10^{-26}	2.170172×10^{-06}	0.215
17	1.318535×10^{-36}	1.781969×10^{-29}	7.399313×10^{-08}	0.217
19	1.493551×10^{-41}	6.981316×10^{-33}	2.139354×10^{-09}	0.218
21	1.459820×10^{-46}	2.745186×10^{-36}	5.317744×10^{-11}	0.537

^aThe values are presented with six significant digits. The integration is designed with five significant digits.

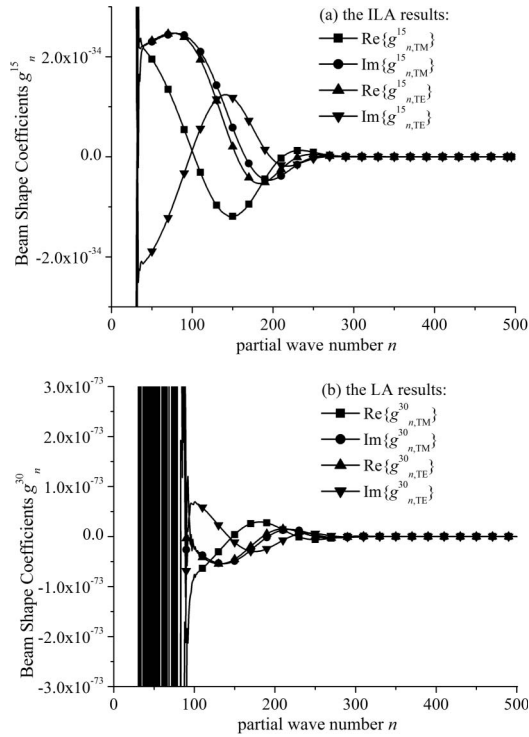


Fig. 4. Results of \bar{g}_n^1 computed by (a) the LA and (b) ILA for $\lambda = 0.5145 \mu\text{m}$, $\omega_{0x} = 3 \text{ mm}$, $\omega_{0y} = 2 \mu\text{m}$, $x_0 = y_0 = 5 \mu\text{m}$, and $z_0 = 0.2 \text{ mm}$.

to compute the Bessel functions multiplying by a prefactor. Notably, we compute $e^{-|\text{Im}(F)|}J_p(F)$ and $e^{-|\text{Im}(\bar{D})|}J_p(\bar{D})$ instead of the direct computation of the Bessel functions. As the corresponding compensation, we compute $e^{|\text{Im}(F)|+|\text{Im}(\bar{D})|}Z_n^m$ instead of Z_n^m .

In addition, we should point out that, since the BSCs can be formulated into the Bessel functions as we have presented in Eq. (29) and the Bessel function can be expanded into the Taylor series, the triple summations derived in [25] contain such Taylor series. And we have known that the Taylor series expansion of the Bessel function $J_p(u)$ is of low convergence when $|u| > 2\sqrt{p}$. Therefore, it is not difficult to understand that the triple summations in the LA lacks stability in numerical computation of the BSCs and the compact formulation of the BSCs presented in this paper can avoid such a disadvantage.

Numerical computations are also performed with the parameters $\lambda = 0.5145 \mu\text{m}$, $\omega_{0x} = 3 \text{ mm}$, $\omega_{0y} = 2 \mu\text{m}$, $x_0 = y_0 = 5 \mu\text{m}$, and $z_0 = 0.2 \text{ mm}$. The azimuthal number m increases from 0 to 50 and the partial wave number n changes from m to 500. The LA calculation is able to obtain reasonable results and the computational speed does not change visibly. The CPU time for a run of a single BSC is about 0.06 ms on average. However, the ILA calculation starts to break down when $m \geq 15$. An example is shown in Fig. 4. The BSCs calculated with the ILA are incorrect for those $m \approx n$ and this becomes more serious when m increases further.

Further evaluation of the BSCs with the proposed LA formulation is implemented for the elliptical Gaussian beam of

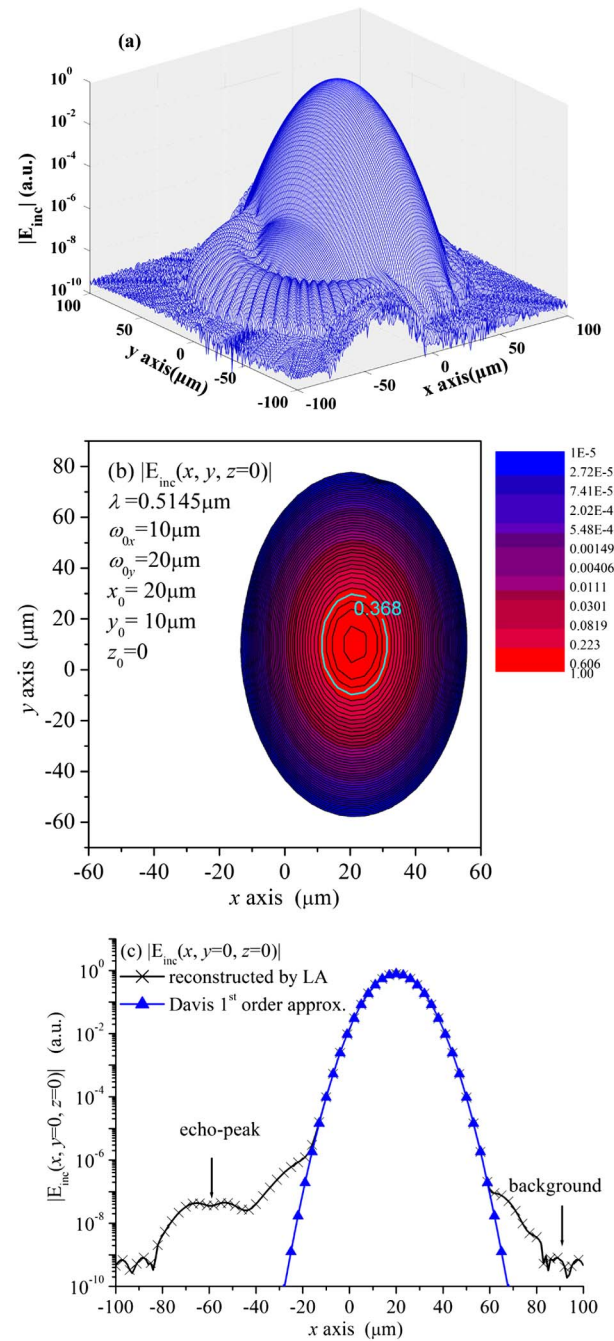


Fig. 5. Beam profile reconstructed with the localized approximation. (a) 3D surface plot, (b) the contour, and (c) a comparison between the reconstructed profile and the Davis first-order beam approximation along the x -axis.

parameters $\lambda = 0.5145 \mu\text{m}$, $\omega_{0x} = 5 \mu\text{m}$, and $\omega_{0y} = 10 \mu\text{m}$. The results are identical to those of [25] and very close to the BSCs evaluated by using the quadrature method.

In Fig. 5, the electric field of the incident elliptical Gaussian beam in the waist plane is reconstructed by using the BSCs computed with the LA method. The beam center is located at $x_0 = 20 \mu\text{m}$ and $y_0 = 10 \mu\text{m}$. The radii of the beam waist are $\omega_{0x} = 10 \mu\text{m}$ and $\omega_{0y} = 20 \mu\text{m}$ along the x - and y -axes. The surface plot of Fig. 5(a) shows the dominant part of the

elliptical Gaussian beam, the echo-peaks at the low level, and the background. In Fig. 5(b), only the dominant part of the beam ranging from 10^{-5} to 1 is plotted. The 0.368 level corresponds to the widths of the beam. Figure 5(c) makes a comparison between the reconstructed field and the original elliptical Gaussian beam along the x -axis. The reconstructed field is identical to the Davis first-order approximation of the original beam in the range of $|x - x_0| \leq 3\omega_{0x}$. The LA produces tiny echo-peak outside the dominated part of the beam, as shown in Figs. 5(a)–5(c) [16,17]. The background at the level of 10^{-9} is caused by the round-off errors in the numerical computation.

4. CONCLUSION

In this work, we obtain a compact formulation of the beam-shape coefficients for an elliptical Gaussian beam, which is given in terms of the Bessel functions. The formulation exhibits good properties of speed, reliability, and stability in numerical computation, compared with the expanded expression (i.e., multiple summations of series) and the integral localized approximation. With this formulation, the beam profile can be reconstructed satisfactorily for the dominated part of the elliptical Gaussian beam. Numerical computation is implemented in the frame of the OLA but the proposed formulation is also applicable to the MLA with slight modification.

Funding. National Natural Science Foundation of China (NSFC) (NSFC 51476104); Shanghai Key Lab of Modern Optical System.

Acknowledgment. The work is supported by the NSFC (NSFC 51476104) and partly supported by Shanghai Key Lab of Modern Optical System.

REFERENCES

- G. Gréhan and G. Gouesbet, "Optical levitation of a single particle to study the theory of the quasi-elastic scattering of light," *Appl. Opt.* **19**, 2485–2487 (1980).
- J. A. Lock and G. Gouesbet, "Generalized Lorenz–Mie theory and applications," *J. Quant. Spectrosc. Radiat. Transfer* **110**, 800–807 (2009).
- G. Gouesbet, "Generalized Lorenz–Mie theories, the third decade: a perspective," *J. Quant. Spectrosc. Radiat. Transfer* **110**, 1223–1238 (2009).
- G. Gouesbet and G. Gréhan, in *Generalized Lorenz–Mie Theories* (Springer, 2011).
- G. Gouesbet, "Latest achievements in generalized Lorenz–Mie theories: a commented reference database," *Ann. Phys.* **526**, 461–489 (2014).
- G. Gouesbet and J. A. Lock, "On the description of electromagnetic arbitrary shaped beams: the relationship between beam shape coefficients and plane wave spectra," *J. Quant. Spectrosc. Radiat. Transfer* **162**, 18–30 (2015).
- G. Gouesbet and J. A. Lock, "On the electromagnetic scattering of arbitrary shaped beams by arbitrary shaped particles: a review," *J. Quant. Spectrosc. Radiat. Transfer* **162**, 31–49 (2015).
- G. Gouesbet, B. Maheu, and G. Gréhan, "Light scattering from a sphere arbitrarily located in a Gaussian beam using a Bromwich formulation," *J. Opt. Soc. Am. A* **5**, 1427–1443 (1988).
- B. Maheu, G. Gouesbet, and G. Gréhan, "A concise presentation of the generalized Lorenz–Mie theory for arbitrary location of the scatterer in an arbitrary incident profile," *J. Opt.* **19**, 59–67 (1988).
- G. Gouesbet, C. Letellier, K. F. Ren, and G. Gréhan, "Discussion of two quadrature methods of evaluating beam-shape coefficients in generalized Lorenz–Mie theory," *Appl. Opt.* **35**, 1537–1542 (1996).
- G. Gouesbet, G. Gréhan, and B. Maheu, "Computations of the g_n^m coefficients in the generalized Lorenz–Mie theory using three different methods," *Appl. Opt.* **27**, 4874–4883 (1988).
- G. Gouesbet, G. Gréhan, and B. Maheu, "Expressions to compute the coefficients g_n^m in the generalized Lorenz–Mie theory using finite series," *J. Opt.* **19**, 35–48 (1988).
- G. Gouesbet, G. Gréhan, and B. Maheu, "On the generalized Lorenz–Mie theory: first attempt to design a localized approximation to the computation of the coefficients g_n^m ," *J. Opt.* **20**, 31–43 (1989).
- G. Gouesbet, G. Gréhan, and B. Maheu, "Localized interpretation to compute all the coefficients g_n^m in the generalized Lorenz–Mie theory," *J. Opt. Soc. Am. A* **7**, 998–1007 (1990).
- K. F. Ren, G. Gréhan, and G. Gouesbet, "Localized approximation of generalized Lorenz–Mie theory: faster algorithm for computation of the beam shape coefficients, g_n^m ," *Part. Part. Syst. Charact.* **9**, 144–150 (1992).
- J. A. Lock and G. Gouesbet, "Rigorous justification of the localized approximation to the beam-shape coefficients in generalized Lorenz–Mie theory, I: on-axis beams," *J. Opt. Soc. Am. A* **11**, 2503–2515 (1994).
- G. Gouesbet and J. A. Lock, "Rigorous justification of the localized approximation to the beam-shape coefficients in generalized Lorenz–Mie theory, II: off-axis beams," *J. Opt. Soc. Am. A* **11**, 2516–2525 (1994).
- J. A. Lock, "Improved Gaussian beam-scattering algorithm," *Appl. Opt.* **34**, 559–570 (1995).
- G. Gouesbet, "Validity of the localized approximation for arbitrary shaped beams in the generalized Lorenz–Mie theory for spheres," *J. Opt. Soc. Am. A* **16**, 1641–1650 (1999).
- G. Gouesbet, J. A. Lock, and G. Gréhan, "Generalized Lorenz–Mie theories and description of electromagnetic arbitrary shaped beams: localized approximations and localized beam models, a review," *J. Quant. Spectrosc. Radiat. Transfer* **112**, 1–27 (2011).
- G. Gouesbet, "Second modified localized approximation for use in generalized Lorenz–Mie theory and other theories revisited," *J. Opt. Soc. Am. A* **30**, 560–564 (2013).
- G. Gouesbet and J. A. Lock, "Comments on localized and integral localized approximations in spherical coordinates," *J. Quant. Spectrosc. Radiat. Transfer* **179**, 132–136 (2016).
- K. F. Ren, G. Gouesbet, and G. Gréhan, "Integral localized approximation in generalized Lorenz–Mie theory," *Appl. Opt.* **37**, 4218–4225 (1998).
- G. Gouesbet and J. A. Lock, "List of problems for future research in generalized Lorenz–Mie theories and related topics, review and prospectus," *Appl. Opt.* **52**, 897–916 (2013).
- K. F. Ren, G. Gréhan, and G. Gouesbet, "Evaluation of laser-sheet beam shape coefficients in generalized Lorenz–Mie theory by use of a localized approximation," *J. Opt. Soc. Am. A* **11**, 2072–2079 (1994).
- R. Li, C. Ding, K. F. Ren, X. Han, L. Guo, Z. Wu, and S. Gong, "Scattering of a high-order Bessel beam by a sphere, in *International Symposium on Antennas, Propagation, and EM Theory (ISAPET)* (IEEE, 2012), Vol. **8543**, pp. 833–836.
- L. A. Ambrosio and H. E. Hernández-Figueroa, "Integral localized approximation description of v -th order Bessel beams in the generalized Lorenz–Mie theory and applications to optical trapping," in *PIERS Proceedings*, Marrakesh, Morocco, March 20–23, 2011.
- W. Zeng, M. Xu, Y. Zhang, and Z. Wang, "Laser sheet drop sizing of evaporating sprays using simultaneous LIEF/MIE techniques," *Proc. Combust. Inst.* **34**, 1677–1685 (2013).
- A. A. Naqwi, X. Liu, and F. Durst, "Evaluation of the dual-cylindrical wave laser technique for sizing of liquid droplets," *Part. Part. Syst. Charact.* **9**, 44–51 (1992).
- V. Garces-Chavez, D. McGloin, H. Melville, W. Sibbett, and K. Dholakia, "Simultaneous micromanipulation in multiple planes using a self-reconstructing light beam," *Nature* **419**, 145–147 (2002).

31. D. Grier, "A revolution in optical manipulation," *Nature* **424**, 810–816 (2003).
32. K. F. Ren, G. Gréhan, and G. Gouesbet, "Electromagnetic field expression of a laser sheet and the order of approximation," *J. Opt.* **25**, 165–176 (1994).
33. J. J. Wang and G. Gouesbet, "Note on the use of localized beam models for light scattering theories in spherical coordinates," *Appl. Opt.* **51**, 3832–3836 (2012).
34. M. Abramowitz and I. A. Stegun, in *Handbook of Mathematical Functions* (National Bureau of Standards, 1972).
35. C. F. du Toit, "The numerical computation of Bessel functions of the first and second kind for integer orders and complex arguments," *IEEE Trans. Antennas Propag.* **38**, 1341–1349 (1990).
36. C. F. du Toit, "Bessel functions and for integer order and complex argument," *Comput. Phys. Commun.* **78**, 181–189 (1993).
37. C. F. du Toit, "Evaluation of some algorithms and programs for the computation of integer-order Bessel functions of the first and second kind with complex arguments," *IEEE Antennas Propag. Mag.* **35**(3), 19–25 (1993).